

Halocline water modification and along slope advection

D. Bauch et al.

This discussion paper is/has been under review for the journal Ocean Science (OS).
Please refer to the corresponding final paper in OS if available.

Halocline water modification and along slope advection at the Laptev Sea continental margin

**D. Bauch¹, S. Torres-Valdes², I. Polyakov³, A. Novikhin⁴, I. Dmitrenko⁵,
J. McKay⁶, and A. Mix⁶**

¹GEOMAR Helmholtz Centre for Ocean Research Kiel, Wischhofstr. 1–3, 24148 Kiel, Germany

²Ocean Biogeochemistry and Ecosystems, National Oceanography Centre (NOC), European Way, Southampton, SO14 3ZH, UK

³International Arctic Research Center and College of Natural Science and Mathematics, University of Alaska Fairbanks, Fairbanks, Alaska

⁴Arctic and Antarctic Research Institute, St. Petersburg, Russia

⁵Centre for Earth Observation Science, University of Manitoba, Winnipeg, Manitoba, Canada

⁶College of Earth, Ocean and Atmospheric Sciences, Oregon State University, Corvallis, Oregon, USA

Title Page

Abstract

Introduction

Conclusions

References

Tables

Figures

⏪

⏩

◀

▶

Back

Close

Full Screen / Esc

Printer-friendly Version

Interactive Discussion

Received: 23 August 2013 – Accepted: 7 September 2013 – Published: 12 September 2013

Correspondence to: D. Bauch (dbauch@geomar.de)

Published by Copernicus Publications on behalf of the European Geosciences Union.

OSD

10, 1581–1617, 2013

**Halocline water
modification and
along slope
advection**

D. Bauch et al.

Title Page

Abstract

Introduction

Conclusions

References

Tables

Figures



Back

Close

Full Screen / Esc

Printer-friendly Version

Interactive Discussion



Abstract

A general pattern in water mass distribution and potential shelf-basin exchanges is revealed at the Laptev Sea continental slope based on hydrochemical and stable oxygen isotope data from summers 2005–2009. Despite considerable interannual variations, a frontal system can be inferred between shelf, continental slope and central Eurasian Basin waters in the upper 100 m of the water column along the continental slope. Net sea-ice melt is consistently found at the continental slope; however the sea-ice melt-water signal is independent from the local retreat of the ice cover and appears to be advected from upwind locations.

In addition to the along-slope frontal system at the continental shelf break a strong gradient is identified on the Laptev Sea shelf between 122 and 126° E with an eastward increase of riverine and sea-ice related brine water contents. These waters cross the shelf break at ~ 140° E and feed the Low Salinity Halocline Water (LSHW, salinity $S < 33$) in the upper 50 m of the water column. Extremely high silicate concentrations in Laptev Sea bottom waters may lead to speculation on a link to the local silicate maximum found within the salinity range of ~ 33 to 34.5, typical for the Lower Halocline Water (LHW) at the continental slope. But brine signatures and nutrient ratios from the central Laptev Sea differ from those at the continental slope. Thus a significant contribution of Laptev Sea bottom waters to the LHW at the continental slope can be excluded. The silicate maximum within the LHW at the continental slope may be formed locally or at the outer Laptev Sea shelf. Similar to the advection of the sea-ice melt signal along the Laptev Sea continental slope the nutrient signal at 50–70 m water depth within the LHW might also be fed by advection parallel to the slope. Thus, our analyses suggest that advective processes from upwind locations play a significant role in the halocline formation in the northern Laptev Sea.

Halocline water modification and along slope advection

D. Bauch et al.

Title Page

Abstract

Introduction

Conclusions

References

Tables

Figures



Back

Close

Full Screen / Esc

Printer-friendly Version

Interactive Discussion



1 Introduction

Numerous changes are predicted for the Arctic environment in the near future: Models suggest that the permanent Arctic sea-ice cover may evolve to seasonal within the next few decades (e.g. Overland and Wang, 2013) affecting also the perennial sea-ice dynamics on the Arctic shelves. In addition, precipitation and the freshwater load from rivers may increase (Zhang et al., 2013). Impact of these and other processes related to and defining high-latitude freshwater balances may be critical for the state of the Arctic halocline, which is a ~ 150 m thick layer with typical temperatures close to freezing and salinities sharply increasing with depth. The halocline insulates the Arctic sea-ice cover from impact of underlying Atlantic Water heat due to its strong stratification, thus playing a fundamental climatological role (Rudels et al., 1996). Hence, in light of climate change and its potential impacts on the Arctic Ocean halocline, further knowledge is needed on its current structure and the processes and regions involved in its formation.

The so-called Lower Halocline Water (LHW) is formed in the Eurasian sector of the Arctic Ocean by modification of Atlantic Water over the Barents and northern Kara seas (Aagaard et al., 1981; Steele and Boyd, 1998; Rudels, 2004) and near the continental slope north of Svalbard (Rudels, 2004). The LHW has salinities of about ~ 33 to 34.5 and is close to the freezing point of sea-water. Only near the continental margin temperatures of LHW are slightly higher (Dmitrenko et al., 2011). Overlying the LHW are low-salinity halocline waters, referred to as Low-Salinity Halocline Water (LSHW), with salinities < 33. LSHW contains large quantities of Siberian river water and originate either in the Laptev Sea (Bauch et al., 2009, 2011b) or in the East Siberian Sea (Anderson et al., 2013). The salinity of shelf waters is variable and relatively low, while temperature may vary from close to the freezing point to seasonally high temperatures of up to 5 °C. Therefore shelves are not only a source of freshwater but potentially also a source of heat which may become increasingly important as summer sea ice extent continues to decrease.

Halocline water modification and along slope advection

D. Bauch et al.

Title Page

Abstract

Introduction

Conclusions

References

Tables

Figures



Back

Close

Full Screen / Esc

Printer-friendly Version

Interactive Discussion



Halocline water modification and along slope advection

D. Bauch et al.

Title Page

Abstract

Introduction

Conclusions

References

Tables

Figures

⏪

⏩

◀

▶

Back

Close


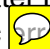
Full Screen / Esc

Printer-friendly Version

Interactive Discussion

2009 (YS09) (see expedition reports in Kassens and Volkmann-Lark, 2010). Water samples were in all cases taken with a conductivity-temperature-depth (CTD)-rosette with an accuracy of at least $\pm 0.002 \text{ S m}^{-1}$ in conductivity and $\pm 0.005 \text{ }^\circ\text{C}$ in temperature.

Our measurement precision for all presented $\delta^{18}\text{O}$ is at least $\pm 0.04 \text{ }‰$ (Bauch et al., 2010, 2011a, b, 2013). All $^{18}\text{O}/^{16}\text{O}$ ratios were calibrated with VSMOW and reported in the usual δ -notation (Craig, 1961). The NABOS stable isotope data from 2008 and 2009 data are presented for the first time. Both datasets were analyzed at the Stable Isotope Laboratory of CEOAS at Oregon State University (Corvallis, USA) applying the CO_2 -water isotope equilibration technique and analyzed by dual inlet mass spectrometry on a DeltaPlus XL. Laptev Sea data for 2008 and 2009 are published in Bauch et al. (2013). Data from NABOS 2005 and 2006 were published in condensed form in Bauch et al. (2011a). Data taken on three expeditions in 2007 (IP07, VB07, PS07) were published separately for the basin (Bauch et al., 2011b) and the shelf (Bauch et al., 2010).

NABOS 2005 and 2006 water samples for silicate (here after referred to as Si), total nitrate ($\text{NO}_3 + \text{NO}_2$, hereafter referred to as ) and phosphate (hereafter referred to as P) were collected in 50 mL plastic bottles and frozen at -20°C until analysis. Analyses were carried out within one month with photometric techniques using a SKALAR Sun Plus nutrient autoanalyzer (in range: 2–100 ppb) at the Otto-Schmidt Laboratory (St. Petersburg, Russia) following “Skalar” methods (US Environmental Protection Agency, 1983). Data from 2005 show a systematic deviation from the Atlantic Water N/P correlation (Jones et al., 1998; see Fig. 8) that we believe to be a systematic  or possibly due to incomplete reduction of NO_3 to NO_2 during analysis. During NABOS 2007 and 2008, Si, N and P were analysed within 30 min of sample collection using a continuous-flow Skalar San plus autoanalyser. Precision based on standard measurements and randomly selected replicates showed a variation of $< 3.5 \text{ }‰$ from mean concentrations (for further details see NABOS expedition reports). During NABOS 2009 samples were analysed on board for Si, N and P using colorimetric methods following Bordovsky and

Ivanenkov (1992), and VNIRO (1998). Quality of N and P data for this 2009 data set is bad and thus are not used here.

3 Mass balance analysis of freshwater sources

Based on a $\delta^{18}\text{O}$ and salinity mass balance, the different freshwater sources can be separated. The major freshwater sources are river water and sea-ice meltwater (SIM), both of which originate mainly on the Arctic shelf areas. Freshwater fractions in each water sample can be estimated using mass balance calculations as was previously done in the central Arctic Ocean (e. g., Östlund and Hut, 1984; Bauch et al., 1995; Ekwurzel et al., 2001; Yamamoto-Kawai et al., 2008) and shelf regions (Macdonald et al., 1995, Cooper et al., 1997; Bauch et al., 2005). It is assumed that each summer sample is a mixture between Atlantic derived water (f_{mar}), river runoff (f_r), and sea-ice meltwater (f_{SIM}). The mass balance is governed by the following equations:

$$f_{\text{mar}} + f_r + f_{\text{SIM}} = 1, \quad (1)$$

$$f_{\text{mar}} \cdot S_{\text{mar}} + f_r \cdot S_r + f_{\text{SIM}} \cdot S_{\text{SIM}} = S_{\text{meas}}, \quad (2)$$

$$f_{\text{mar}} \cdot O_{\text{mar}} + f_r \cdot O_r + f_{\text{SIM}} \cdot O_{\text{SIM}} = O_{\text{meas}}, \quad (3)$$

where f_{mar} , f_r , and f_{SIM} are the fractions of marine water, river runoff, and sea-ice meltwater in a water parcel, and S_{mar} , S_r , S_{SIM} , O_{mar} , O_r and O_{SIM} are the corresponding salinities and $\delta^{18}\text{O}$ values (Tab. 1). S_{meas} and O_{meas} are the measured salinity and $\delta^{18}\text{O}$ of the water samples. For further details on the selection of end-members applicable for the Laptev Sea and the Eurasian Basin regions refer to Bauch et al. (2010, 2011b). As only stations west of 150°E are discussed no additional analysis for the influence of Pacific derived waters is necessary (Abrahamsen et al., 2009; Bauch et al., 2011b).

Halocline water modification and along slope advection

D. Bauch et al.

Title Page

Abstract

Introduction

Conclusions

References

Tables

Figures

◀

▶

◀

▶

Back

Close

Full Screen / Esc

Printer-friendly Version

Interactive Discussion



Halocline water modification and along slope advection

D. Bauch et al.

Title Page

Abstract

Introduction

Conclusions

References

Tables

Figures

⏪

⏩

◀

▶

Back

Close

Full Screen / Esc

Printer-friendly Version

Interactive Discussion



All fractions are net values reconstructed from the $\delta^{18}\text{O}$ and salinity signatures of each sample, and reflect the time-integrated effects on the sample volume over the residence time of the water. Negative SIM fractions (f_{SIM}) reflect the amount of water removed by sea ice formation and are proportional to the subsequent addition of brines to the remaining water column. SIM fractions may be negative during summer season sampling if the winter signal exceeds the summer signal. The analytical errors that arise from $\delta^{18}\text{O}$ and salinity measurements add up to $\sim 0.3\%$ for each of the fractions. An additional systematic error depends on the exact choice of end-member values. When end-member values are varied within the estimated uncertainties (Table 1), both fractions are shifted by up to $\sim 1\%$ in absolute values, but results are always qualitatively conserved even when extreme variations in end-member values are tested (see Bauch et al., 2011b).

Inventories of river water and sea-ice meltwater were calculated by integrating each fraction from surface down to 150 m or bottom depth. As most of the river water and sea-ice meltwater are found within the upper 50–100 m water depth, the choice of the integration depth is not critical to relative values, but rather adds a systematic offset. When an integration depth of 100 m is chosen instead of 150 m the offset in both fractions is generally below 15% of the total inventory value and is below $\sim 0.7\text{ m}$ and $\sim 0.3\text{ m}$ in river and sea-ice inventory values respectively. Integration depths on the shelf are mostly at $\sim 50\text{ m}$ water depth or smaller but there is no systematic trend in river and sea-ice inventory values with bottom depth. Inventory values represent the thickness of the water column consisting of pure river water or sea-ice meltwater. Negative inventory values for sea-ice meltwater represent the thickness of the water removed from the water column as sea ice.

4 Results

Along the Laptev Sea continental margin $\delta^{18}\text{O}$ and salinity show a first order linear correlation and strong interannual variations (Fig. 2). Low salinity ($\sim 26\text{--}28$) waters

Halocline water modification and along slope advection

D. Bauch et al.

Title Page

Abstract

Introduction

Conclusions

References

Tables

Figures

⏪

⏩

◀

▶

Back

Close

Full Screen / Esc

Printer-friendly Version

Interactive Discussion

are found in 2005 and 2007 only. Sampling in 2007 captures low salinity shelf waters with stations taken relatively far south ($\sim 74^\circ\text{N}$) onto the central shelf (see Fig. 1), explaining the observed low salinities within the 2007 NABOS and Polarstern dataset. In 2005 low salinities between ~ 26 – 28 were found at $\sim 142^\circ\text{E}$ close to the continental slope where a cross-slope section was sampled in all years (Fig. 1). However, only 2005 observations at $\sim 142^\circ\text{E}$ showed such low salinities and corresponding low $\delta^{18}\text{O}$ values (Fig. 2) which can be linked to enhanced export of central Laptev Sea shelf waters in this year.

The oceanographic section at $\sim 126^\circ\text{E}$ documents the interannual variability across the continental margin from the central Laptev Sea to the deep basin (Fig. 5). Relatively fresh and warm surface waters containing high river water fractions (f_r) with maximum values at the surface can be seen to a variable extent over the Laptev Sea shelf in all years. In the upper 50 m of the water column salinity increases from the shelf break towards the basin, and river water fractions decrease accordingly. The calculated sea-ice meltwater fractions are mostly negative for shelf waters. Sea-ice related brine signals (negative f_{SIM}) are in general largest in the bottom layer with the exception of summer 2007, when they were largest near the surface (see for details Bauch et al., 2010). Negative f_{SIM} signals in the basin are generally lower than on the shelf, but show a distinct maximum at about 30 to 50 m water depth off the shelf break. A thin surface layer of sea-ice meltwater (positive f_{SIM}) extends from the basin, over the shelf break and partly onto the shelf (subject to an inter-annual variations) southwards to ~ 77 – 75°N (Fig. 3). The distribution of silicate shows a maximum over the shelf within the low salinity surface layer and a second maximum at the bottom over the shelf. At the shelf break there is a discontinuity visible in temperature and the sea-ice related brine signal, located at about 30–50 m (Fig. 3; at 126°E , $\sim 77^\circ\text{N}$). Silicate values are low off the shelf break but show a maximum at the bottom directly at the shelf break (Fig. 3, at ~ 50 – 70 m depth and $\sim 76.7^\circ\text{N}$; see also Table 2).

In summer 2007, oceanographic cross-slope sections were taken at $\sim 122^\circ\text{E}$, 126°E , 130°E and $\sim 142^\circ\text{E}$ (Fig. 4). This quasi-synoptic view of water masses at the continen-

at the Laptev Sea shelf break (Fig. 7) shows two clusters that can be assigned to waters formed in either (i) coastal polynyas, with high f_r and low salinities, or (ii) polynyas near the continental slope or in open ocean with relatively low f_r and relatively high salinities (Bauch et al., 2011b). The f_{SIM}/f_r correlation with extremely low river water fractions is not visible off the continental slope of the western Laptev Sea (Fig. 7, see orange circles). This is consistent with the export of brine-enriched bottom waters originating in Laptev Sea coastal polynyas that occurs via the easternmost part of the Laptev Sea (Bauch et al., 2009) not continuously but in pulses (Bauch et al., 2011a, b; Karcher et al., 2006) in response to atmospheric forcing (Guay et al., 2001; Dmitrenko et al., 2008; Bauch et al., 2011a). Nevertheless, river water fractions in surface waters of the western Laptev Sea continental slope are still up to $\sim 8\%$ (at $S \sim 32-34$) and $\sim 15\%$ (at $S \sim 31-29$) (Fig. 7). Where do these signals come from given the general eastward advection in this area? It is known that Ob and Yenisei river water does not leave the Kara Sea northwards but flows around Taymyr Peninsula directly through Vilkitsky Strait into the northwestern Laptev Sea (Bauch et al., 2011b). Hence, the river water found in surface waters at the continental slope of the western Laptev Sea is likely entirely Ob and Yenisei river water.

5.2 Relation between sea-ice melt and ice edge

At the continental slope of the western and central Laptev Sea, SIM fractions are mostly positive and reflect a surplus of sea-ice melt in the area (Fig. 7, see orange circles). All SIM fractions are net signals. Therefore a negative f_{SIM} from the winter season may be “overwritten” by sea-ice melt of the current summer season. As Arctic shelves are regions of sea-ice export SIM values remain largely negative here also during summer (Bauch et al., 2005). On the Laptev Sea shelf the retreat of the seasonal ice cover is governed by wind forcing (Bareiss et al., 1999) and sea-ice melt is found only in correlation with elevated river water fractions in years with a pronounced river plume (Bauch et al., 2013). Therefore sea-ice melt on the shelf may originate solely from initial breakup of the fast-ice (Bauch et al., 2013) triggered by the river plume in the

Halocline water modification and along slope advection

D. Bauch et al.

Title Page

Abstract

Introduction

Conclusions

References

Tables

Figures



Back

Close

Full Screen / Esc

Printer-friendly Version

Interactive Discussion



Halocline water modification and along slope advection

D. Bauch et al.

Title Page

Abstract

Introduction

Conclusions

References

Tables

Figures

⏪

⏩

◀

▶

Back

Close

Full Screen / Esc

Printer-friendly Version

Interactive Discussion



southeastern Laptev Sea (Bareiss et al., 1999). In contrast to the shelf, positive f_{SIM} are generally observed in surface waters at the Laptev Sea continental slope (Fig. 3). SIM inventory values along the western and central continental slope are consistently positive in all years (Fig. 5), while they are mostly negative north and south of the shelf break (Fig. 5). At the eastern Laptev Sea continental slope, SIM inventories are consistently negative because waters with a surplus of sea-ice related brines (negative f_{SIM}) leave the shelf through this region (Bauch et al., 2009, 2011b).

The minimum of Arctic ice cover occurs around mid September and is reflected by the highly variable location of the ice edge at this time (Fig. 5). Because sampling in all years was conducted in September close to the general minimum of the summer ice extent, a maximal input of sea-ice melt to surface waters can be expected from the current summer season and should be reflected in considerable sea-ice melt contributions (positive SIM) at the surface at and south of the ice edge. Surprisingly the ice edge on 15 September shows no apparent correlation or pattern with SIM inventory values (Fig. 5). This indicates that the general decay of the sea-ice cover near the continental slope is not primarily controlled by local sea-ice melting. A single station taken near Severnaya Zemlya in 2009 shows a 34 m thick low salinity layer with 28–30 % sea-ice meltwater (see Fig. 7). Such a pronounced locally restricted meltwater layer is likely strongly influenced by local melting. But positive SIM inventory values are found even below the ice cover north of Severnaya Zemlya in 2006 (Fig. 5). It therefore seems reasonable to argue that the positive SIM signal along the western and central Laptev Sea continental margin is not determined by local melting but it is to a large degree determined by lateral advection of waters within the halocline and the upper 50 m along the continental slope from west to east, from the northern Kara Sea or the Barents Sea. Such an advection is consistent with a shelf break branch of the Arctic Continental Boundary Current (Aksenov et al., 2011; Dmitrenko et al., 2012).

5.3 Laptev Sea export of silicate and N/P signatures

Extremely high silicate concentrations are observed on the Laptev Sea shelf (Fig. 3). The silicate maximum found at the bottom on the continental slope within the salinity range of the LHW could therefore originate from an admixture of these high silicate bottom waters from the Laptev Sea (Dmitrenko et al., 2011). In the following chapter this hypothesis will be further discussed.

The Lena River has extremely high silicate concentrations (Si) with up to 4 mg Si L^{-1} ($\sim 140 \mu\text{mol L}^{-1}$), similar to high silicate and nutrient values of most Arctic rivers such as the Ob and Yenisei (Holmes et al., 2012). Due to the relative excess of silicate, biological processes in the Laptev Sea are limited by nitrate (N) and phosphate (P). Once N and P are depleted, high Si concentrations still remain in waters with high fractions of river water. Si is therefore a **good indicator for Lena River** water within the surface layer (Wegner et al., 2013; Pivovarov et al., 2004). But Si as well as N and P concentrations show also a local maximum at the bottom within the Laptev Sea bottom layer (Pivovarov et al., 2004; see also Si within Fig. 3, N and P not shown). High nutrient concentrations at depth result from remineralisation and dissolution of sinking particles, as well as from resuspension at the sediment-water interface (Santschi et al., 1990). This nutrient regeneration explains the coincident distribution of the maxima of Si and the sea-ice related brine signal (negative SIM) within the Laptev Sea bottom layer even though the processes that produce each signal are clearly different. That is, the Si and nutrient maxima within the bottom layer likely originate at the sediment-water interface, possibly over the entire Laptev Sea shelf and slope area. The signal of sea-ice related brine (negative SIM) is instead introduced to the whole water column within the polynya region (Fig. 1) on the central Laptev Sea shelf during winter. Within the bottom layer however, this brine signal remains unaltered by surface summer processes (Bauch et al., 2013). In fact, the Si maxima found at 126° E near the bottom of the continental slope are not accompanied by a significant sea-ice related brine signal (negative SIM; Fig. 3). The brine signal on the central Laptev Sea shelf

Halocline water modification and along slope advection

D. Bauch et al.

Title Page

Abstract

Introduction

Conclusions

References

Tables

Figures

⏪

⏩

◀

▶

Back

Close

Full Screen / Esc

Printer-friendly Version

Interactive Discussion

largely ceases at the continental slope, slightly further south of the Si maxima (Fig. 3). An exception is the Si maximum observed in 2005 together with a pronounced negative SIM signal and relatively high salinity of $S \sim 33.5$. In all years the observed Si values of $\sim 10 \mu\text{mol L}^{-1}$ within the maxima at the continental slope (Table 2) are considerably lower than concentrations found in Laptev Sea bottom waters, though are significantly higher than the concentrations of $\sim 6 \mu\text{mol L}^{-1}$ found in the Atlantic Water core within the Eurasian Basin (Bauch et al., 1995). The missing brine signature excludes the central Laptev Sea as the source of the Si maximum that might instead be formed locally at the continental slope, on the outer shelf or it might be advected from the west with the general water transports (e.g. Woodgate et al., 2001; Newton et al., 2008; Aksenov et al., 2011).

The nitrate to phosphate relationship (N/P ratio) can be additionally used as an indicator for the origin of a water mass. N and P usually change at a ratio of $\sim 16 : 1$ (i.e., Redfield ratio) during biological production and remineralisation of organic matter. On the continental shelves this ratio can strongly deviate from the Redfield stoichiometry (e.g. Broecker and Peng, 1980; Nitishinski et al., 2007). In the Arctic Ocean, deviations from the N/P typical of Atlantic waters (Bauch et al., 2011b) are the result of denitrification processes in Pacific derived waters (e.g., Jones et al., 2008; see Fig. 8) and in shelf waters influenced by bottom sediments processes on the Bering and Chukchi shelves (Devol et al., 1997; Tanaka et al., 2004; Yamamoto-Kawai et al., 2006), the East Siberian Sea (Anderson et al., 2013) and in brine-enriched waters flowing off the Laptev Sea shelf (Bauch et al., 2011b). N/P values from systematic sampling campaigns on the Laptev Sea shelf conducted in 2007, 2010, and 2011 strongly deviate from the Atlantic N/P relation within the salinity range of central Laptev Sea bottom waters (Fig. 9a). Denitrification in Laptev Sea bottom waters can be identified using the deviation relative to the Atlantic N/P relation ($N_{\text{Atl}}^* = N - 16.835 \cdot P + 1.918$ after Gruber and Sarmiento, 1997; Fig. 9b). Denitrification N_{Atl}^* occurs mainly on the central Laptev Sea shelf (Fig. 9b).

Halocline water modification and along slope advection

D. Bauch et al.

Title Page

Abstract

Introduction

Conclusions

References

Tables

Figures

◀

▶

◀

▶

Back

Close

Full Screen / Esc

Printer-friendly Version

Interactive Discussion



The N/P signatures observed north of the Laptev Sea continental slope are all close to the Atlantic N/P ratio (Fig. 8), while bottom waters on the Laptev Sea shelf show a signal consistent with denitrification (Figs. 9 and 8, shelf stations). The N/P ratios within the Si maximum at the Laptev Sea continental slope show little or no deviation from the Atlantic N/P line (Fig. 8, pink squares) and therefore give no indication for a potential origin of these waters on the central Laptev Sea shelf. In 2005, when the Si maximum at the central Laptev Sea slope is coincident with a SIM signal, there is also no denitrification signal relative to the overall 2005 N/P ratio (Fig. 8). Only at the eastern continental slope, where the outflow of waters from the central Laptev Sea occurs, the N/P ratios within the Si maximum show a slight denitrification signal in all years (Fig. 8, framed pink squares).

The missing brine contribution within the silicate maximum at the central continental slope excludes the central Laptev Sea shelf as a potential source, where high silicate bottom waters but also high sea-ice related brine signals are found. The N/P signature within the Si maximum at the continental slope (Fig. 8, pink squares) yields no conclusive evidence for the potential origin of these waters within the Laptev Sea.

6 Conclusions

A frontal system is inferred between shelf waters, continental slope waters and basin waters within the Lower Halocline Water (LHW) and Low-Salinity Halocline Water (LSHW) along the continental slope (Fig. 6). $\delta^{18}\text{O}$ -derived signals of river water and sea-ice related brine as well as nutrient ratios (N/P) and signatures from sediment-bottom water denitrification processes (N_{Atl}^*) are found indicative of central Laptev Sea shelf bottom waters and are important for the assignment of shelf, slope and basin water masses of the upper water column along the Laptev Sea continental margin.

Net sea-ice meltwater fractions and inventories show no apparent relationship with the summer ice extent. Instead sea-ice inventories are consistently positive over the continental slope and the summer sea-ice meltwater distribution at the continental margin

Halocline water modification and along slope advection

D. Bauch et al.

Title Page

Abstract

Introduction

Conclusions

References

Tables

Figures

⏪

⏩

◀

▶

Back

Close

Full Screen / Esc

Printer-friendly Version

Interactive Discussion

appears to be influenced by advection from west to east along the Laptev Sea continental slope. In addition to the along-slope frontal system we see a strong zonal gradient on the shelf at $\sim 122\text{--}126^\circ$ E with a sharp increase in river water and sea-ice related brine signal eastward. Both river water and sea-ice related brine waters cross the Laptev Sea shelf break at $\sim 140^\circ$ E, and feed the LSHW with salinities below ~ 33 in the upper 50 m of the water column.

There is no evidence for an entrainment of Laptev Sea shelf waters at higher salinities into the LHW at the Laptev Sea continental margin. The silicate maximum found within the salinity range of LHW at the continental slope cannot originate on the central Laptev Sea shelf as it does not show the typical sea-ice related brine signature. In addition, the nitrate to phosphate ratio (N/P) at the silicate maximum shows no denitrification signal, which is in contrast to central Laptev Sea bottom waters. Our data indicate the silicate maximum and N/P signature at the slope forms either locally, on the outer Laptev Sea shelf, or are advected from elsewhere (Dmitrenko et al., 2011, 2012). Similar to the advection of the sea-ice melt signal along the Laptev Sea continental margin, it seems likely that the silicate signal within the LHW at the continental slope is also fed by lateral advection. Such a lateral advection of water along the continental slope may explain the frontal system between shelf, continental slope and basin that is identified at the central Laptev Sea continental margin (Fig. 6).

With ongoing climate change, considerable alterations within the Laptev Sea shelf environment are to be expected, with likely impact on sea-ice processes. With the potential of further freshening due to increased amounts of river discharge and precipitation (Zhang et al., 2013), the formation mode of brine-enriched bottom waters on the Laptev Sea shelf may be significantly altered (Bauch et al., 2010). With surface freshening, brine-enriched waters are less likely to reach the shelf's bottom layer (Bauch et al., 2012), thus leaving a relatively high salinity bottom layer due to the missing river admixture (Bauch et al., 2010, 2013). Our results thus indicate that with a further freshening, the export of Laptev Sea brine-enriched shelf waters to the Arctic Ocean halocline is to be expected at overall lower salinities and still within LSHW be-

low ~33. Even though salinity in Laptev Sea bottom water potentially increases with surface freshening, whether or not Laptev Sea bottom water reaches the density layer of LHW is less straightforward and further investigations are needed.

Acknowledgements. We thank all members of the NABOS project for exceptional working conditions and extensive support during expeditions. Nutrient data from NABOS expedition in 2009 were provided under the lead of P. Makkakeev (Shirshov Institute, Moscow). Nutrient data in 2007 and 2008 were taken as part of the Natural Environment Research Council (UK) funded Arctic Synoptic Basin-wide Oceanography (ASBO) IPY consortium grant. DB acknowledges funds from the German Research Foundation grants SP 526/3 and BA 1689/2-1 as well as grant 03G0639D funded by the BMBF within the German-Russian cooperation “Laptev Sea System”. AN acknowledges funding through the Federal Ministry of Education and Research project Otto-Schmidt-Laboratory for Polar and Marine Sciences. IP thanks NSF, CIFAR, JAXA and JAMSTERC for support. ID received financial support from the Canadian Excellence Research Chair (CERC) program and also by the BMBF within the German-Russian cooperation “Laptev Sea System” under grant 03G0639A. We thank all colleagues of these projects. Plots were made with Ocean Data View (ODV) (Schlitzer, 2001) and Generic Mapping Tools (GMT) software (Wessel and Smith, 1998).

The service charges for this open access publication have been covered by a Research Centre of the Helmholtz Association.

References

- Aagaard, K., Coachman, L., and Carmack, E.: On the halocline of the Arctic Ocean, *Deep-Sea Res.*, 28, 529–545, 1981.
- Abrahamsen, E. P., Meredith, M. P., Falkner, K. K., Torres-Valdes, S., Leng, M. J., Alkire, M. B., Bacon, S., Laxon, S., Polyakov, I., Ivanov, V., and Kirillov, S.: Tracer-derived freshwater budget of the Siberian Continental Shelf following the extreme Arctic summer of 2007, *Geophys. Res. Lett.*, 36, L07602, doi:10.1029/2009GL037341, 2009.

Halocline water modification and along slope advection

D. Bauch et al.

Title Page

Abstract

Introduction

Conclusions

References

Tables

Figures

◀

▶

◀

▶

Back

Close

Full Screen / Esc

Printer-friendly Version

Interactive Discussion



Halocline water modification and along slope advection

D. Bauch et al.

Title Page

Abstract

Introduction

Conclusions

References

Tables

Figures

⏪

⏩

◀

▶

Back

Close

Full Screen / Esc

Printer-friendly Version

Interactive Discussion

- Aksenov, Y., Ivanov, V. V., Nurser, A. J. G., Bacon, S., Polyakov, I. V., Coward, A. C., Naveira-Garabato, A. C., and Beszczynska-Moeller, A.: The Arctic Circumpolar Boundary Current, *J. Geophys. Res.-Oceans*, 116, C09017, doi:10.1029/2010JC006637, 2011.
- Anderson, L. G., Andersson, P. S., Björk, G., Peter Jones, E., Jutterström, S., and Wåhlström, I.: Source and formation of the upper halocline of the Arctic Ocean, *J. Geophys. Res.-Oceans*, 118, 410–421, doi:10.1029/2012JC008291, 2013.
- Bareiss, J. and Görge, K.: Spatial and temporal variability of sea ice in the Laptev Sea: Analyses and review of satellite passive-microwave data and model results, 1979 to 2002, *Global Planet. Change*, 48, 28–54. doi:10.1016/j.gloplacha.2004.12.004, 2005.
- Bareiss, J., Eicken, H., Helbig, A., and Martin, T.: Impact of river discharge and regional climatology on the decay of sea ice in the Laptev Sea during spring and early summer, *Arct. Antarct. Alp. Res.*, 31, 214–229, 1999.
- Bauch, D., Schlosser, P., and Fairbanks, R. F.: Freshwater balance and the sources of deep and bottom waters in the Arctic Ocean inferred from the distribution of $H_2^{18}O$, *Prog. Oceanogr.*, 35, 53–80, 1995.
- Bauch, D., Erlenkeuser, H., and Andersen, N.: Water mass processes on Arctic shelves as revealed from ^{18}O of H_2O , *Global Planet. Change*, 48, 165–174, doi:10.1016/j.gloplacha.2004.12.011, 2005.
- Bauch, D., Dmitrenko, I. A., Wegner, C., Hölemann, J., Kirillov, S. A., Timokhov, L. A., and Kassens, H.: Exchange of Laptev Sea and Arctic Ocean halocline waters in response to atmospheric forcing, *J. Geophys. Res.-Oceans*, 114, C05008, doi:10.1029/2008JC005062, 2009.
- Bauch, D., Hölemann, J., Andersen, N., Dobrotina, E., Nikulina, A., and Kassens, H.: The Arctic shelf regions as a source of freshwater and brine-enriched waters as revealed from stable oxygen isotopes, *Polarforschung*, 80, 127–140, 2010.
- Bauch, D., Gröger, M., Dmitrenko, I., Hölemann, J., Kirillov, S., Mackensen, A., Taldenkova, E., and Andersen, N.: Atmospheric controlled freshwater water release at the Laptev Sea Continental margin, *Polar Res.*, 30, 5858, doi:10.3402/polar.v30i0.5858, 2011a.
- Bauch, D., Rutgers van der Loeff, M., Andersen, N., Torres-Valdes, S., Bakker, K., and Abrahamsen, E. P.: Origin of freshwater and polynya water in the Arctic Ocean halocline in summer 2007, *Prog. Oceanogr.*, 91, 482–495, doi:10.1016/j.pocean.2011.07.017, 2011b.
- Bauch, D., Hölemann, J. A., Dmitrenko, I. A., Janout, M. A., Nikulina, A., Kirillov, S. A., Krumpfen, T., Kassens, H., and Timokhov, L.: The impact of Siberian coastal polynyas

Halocline water modification and along slope advection

D. Bauch et al.

Title Page

Abstract

Introduction

Conclusions

References

Tables

Figures

◀

▶

◀

▶

Back

Close

Full Screen / Esc

Printer-friendly Version

Interactive Discussion

on shelf-derived Arctic Ocean halocline waters, *J. Geophys. Res.-Oceans*, 117, C00G12, doi:10.1029/2011JC007282, 2012.

Bauch, D., Hölemann, J. A., Nikulina, A., Wegner, C., Janout, M. A., Timokhov, L. A., and Kassens, H.: Correlation of river water and local sea-ice melting on the Laptev Sea shelf (Siberian Arctic), *J. Geophys. Res.-Oceans*, 118, 550–561, doi:10.1002/jgrc.20076, 2013.

Bordovsky, O. K. and Ivanenkov, V. N.: Modern methods of hydrochemical studies of the ocean, IORAS, Moscow, 1992.

Broecker, W. S. and Peng, T. H.: *Tracers in the Sea*, Eldigio, Palisades, NY, 1982.

Cooper, L. W., Whittedge, T. E., Grebmeier, J. M., and Weingartner, T.: The nutrient, salinity, and stable isotope composition of Bering and Chukchi seas waters in and near the Bering Strait, *J. Geophys. Res.*, 102, 12563–12573, 1997.

Cooper, L. W., McClelland, J. W., Holmes, R. M., Raymond, P. A., Gibson, J. J., Guay, C. K., and Peterson, B. J.: Flow-weighted values of runoff tracers ($\delta^{18}\text{O}$, DOC, Ba, alkalinity) from the six largest Arctic rivers, *Geophys. Res. Lett.*, 35, L18606, doi:10.1029/2008GL035007, 2008.

Craig, H.: Standard for reporting concentrations of Deuterium and Oxygen-18 in natural waters, *Science*, 133, 1833–1834, 1961.

Devol, A. H., Codispoti, L. A., and Christensen, J. P.: Summer and winter denitrification rates in western Arctic shelf sediments, *Cont. Shelf Res.*, 17, 1029–1050, doi:10.1016/S0278-4343(97)00003-4, 1997.

Dmitrenko, I. A., Kirillov, S. A., and Tremblay, L. B.: The long-term and interannual variability of summer fresh water storage over the eastern Siberian shelf: Implication for climatic change, *J. Geophys. Res.-Oceans*, 113, C03007, doi:10.1029/2007JC004304, 2008.

Dmitrenko, I. A., Kirillov, S. A., Tremblay, L. B., Bauch, D., Hölemann, J. A., Krumpfen, T., Kassens, H., Wegner, C., Heinemann, G., and Schröder, D.: Impact of the Arctic Ocean Atlantic water layer on Siberian shelf hydrography, *J. Geophys. Res.-Oceans*, 115, C08010, doi:10.1029/2009JC006020, 2010.

Dmitrenko, I. A., Ivanov, V. V., Kirillov, S. A., Vinogradova, E. L., Torres-Valdes, S., and Bauch, D.: Properties of the Atlantic derived halocline waters over the Laptev Sea continental margin: Evidence from 2002 to 2009, *J. Geophys. Res.-Oceans*, 116, C10024, doi:10.1029/2011JC007269, 2011.

Halocline water modification and along slope advection

D. Bauch et al.

Title Page

Abstract

Introduction

Conclusions

References

Tables

Figures

⏪

⏩

◀

▶

Back

Close

Full Screen / Esc

Printer-friendly Version

Interactive Discussion

- Dmitrenko, I. A., Kirillov, S. A., Ivanov, V. V., Rudels, B., Serra, N., and Koldunov, N. V.: Modified Halocline Water over the Laptev Sea Continental Margin: Historical Data Analysis, *J. Climate*, 25, 5556–5565, doi:10.1175/JCLI-D-11-00336.1, 2012.
- Ekwurzel, B., Schlosser, P., Mortlock, R., and Fairbanks, R.: River runoff, sea ice meltwater, and Pacific water distribution and mean residence times in the Arctic Ocean, *J. Geophys. Res.-Oceans*, 106, 9075–9092, 2001.
- Gruber, N. and Sarmiento, J. L.: Global patterns of marine nitrogen fixation and denitrification, *Global Biogeochem. Cy.*, 11, 235–266, 1997.
- Holmes, R., McClelland, J., Peterson, B., Tank, S., Bulygina, E., Eglinton, T., Gordeev, V., Gurtovaya, T., Raymond, P., Repeta, D., Staples, R., Striegl, R., Zhulidov, A., and Zimov, S.: Seasonal and Annual Fluxes of Nutrients and Organic Matter from Large Rivers to the Arctic Ocean and Surrounding Seas, *Estuar. Coast.*, 35, 369–382, doi:10.1007/s12237-011-9386-6, 2012.
- Jones, E., Anderson, L., and Swift, J.: Distribution of Atlantic and Pacific water in the upper Arctic Ocean: Implications for circulation, *Geophys. Res. Lett.*, 25, 765–768, 1998.
- Kassens, H. and Dmitrenko, I. A.: The TRANSDRIFT II expedition to the Laptev Sea, *Rep. Polar Res.*, 182, 1–180., 1995.
- Kassens, H. and Volkmann-Lark, K.: Eurasische Schelfmeere im Umbruch Ozeanische Fronten und Polynjasysteme in der Laptev-See, Sekretariat System Laptev-See, accessible through TIP at <http://opac.tib.uni-hannover.de/DB=1/SET=1/TTL=1/SHW?FRST=1>, 2010.
- Kruppen, T., Janout, M., Hodges, K. I., Gerdes, R., Girard-Ardhuin, F., Hölemann, J. A., and Willmes, S.: Variability and trends in Laptev Sea ice outflow between 1992–2011, *The Cryosphere*, 7, 349–363, doi:10.5194/tc-7-349-2013, 2013.
- Macdonald, W., Paton, D., Carmack, E., and Omstedt, A.: The freshwater budget and under-ice spreading of Mackenzie River water in the Canadian Beauford Sea based on salinity and $^{18}\text{O}/^{16}\text{O}$ measurements in water and ice, *J. Geophys. Res.-Oceans*, 100, 895–919, 1995.
- Melling, H. and Moore, R.: Modification of halocline source waters during freezing on the Beauford Sea shelf: Evidence from oxygen isotopes and dissolved nutrients, *Cont. Shelf Res.*, 15, 89–113, 1995.
- Mueller-Lupp, T., Erlenkeuser, H., and Bauch, H. A.: Seasonal and interannual variability of Siberian river discharge in the Laptev Sea inferred from stable isotopes in modern bivalves, *Boreas*, 32, 292–303, doi:10.1080/03009480310001984, 2003.

Halocline water modification and along slope advection

D. Bauch et al.

Title Page

Abstract

Introduction

Conclusions

References

Tables

Figures

◀

▶

◀

▶

Back

Close

Full Screen / Esc

Printer-friendly Version

Interactive Discussion



Sea shelf during summer, Biogeosciences, 10, 1117–1129, doi:10.5194/bg-10-1117-2013, 2013.

Wessel, P. and Smith, W. H. F.: New improved version of the Generic Mapping Tools released, EOS Trans, AGU, 79, 579, 1998.

5 Woodgate, R. A., Aagaard, K., Muench, R. D., Gunn, J., Björk, G., Rudels, B., Roach, A. T., and Schauer, U.: The Arctic Ocean Boundary Current along the Eurasian slope and the adjacent Lomonosov Ridge: Water mass properties, transports and transformations from moored instruments, Deep-Sea Res. Pt. I, 48, 1757–1792, 2001.

10 Yamamoto-Kawai, M., Carmack, E., and McLaughlin, F.: Nitrogen balance and Arctic through-flow, Nature, 443, 43–43, doi:10.1038/443043a, 2006.

Yamamoto-Kawai, M., McLaughlin, F. A., Carmack, E. C., Nishino, S., and Shimada, K.: Freshwater budget of the Canada Basin, Arctic Ocean, from salinity, $\delta^{18}\text{O}$, and nutrients, J. Geophys. Res.-Oceans, 113, C01007, doi:10.1029/2006JC003858, 2008.

15 Zakharov, V. F.: The role of flaw leads off the edge of fast ice in the hydrological and ice regime of the Laptev Sea, Oceanology, 6, 815–821, 1966.

Zhang, X., He, J., Zhang, J., Polyakov, I., Gerdes, R., Inoue, J., and Wu, P.: Enhanced poleward moisture transport and amplified northern high-latitude wetting trend, Nature Clim. Change, 3, 47–51, doi:10.1038/nclimate1631, 2013.

Halocline water modification and along slope advection

D. Bauch et al.

Title Page

Abstract

Introduction

Conclusions

References

Tables

Figures

◀

▶

◀

▶

Back

Close

Full Screen / Esc

Printer-friendly Version

Interactive Discussion



Table 1. End-Member Values Used in Mass Balance Calculations*.

End-Member	Salinity	$\delta^{18}\text{O}$ (‰)
Marine (f_{mar})	34.92(5)	0.3(1)
River (f_r)	0	-20(1)
Sea ice (f_{SIM})	4(1)	surface + 2.6(1)

* Numbers in parentheses are the estimated uncertainties within the last digit in our knowledge of each end-member value.

Halocline water modification and along slope advection

D. Bauch et al.

Table 2. Station data of Si maximum at the Laptev Sea continental slope. Stations are sorted by area ($\sim 122^\circ\text{E}$, $\sim 126^\circ\text{E}$, $\sim 130^\circ\text{E}$, $\sim 140^\circ\text{E}$). Given that in 2009 no separate Si maximum was observed at the continental margin, no stations are listed for this year.

Cruise	Station	Lon ($^\circ\text{E}$)	Lat ($^\circ\text{N}$)	Bottom [m]	Depth [m]	T [$^\circ\text{C}$]	S [psu]	Si [$\mu\text{mol kg}^{-1}$]	P [$\mu\text{mol kg}^{-1}$]	N [$\mu\text{mol kg}^{-1}$]	$\delta^{18}\text{O}$ [perm.]
PS07	405	122.6	76.7	92	86	-1.33	34.13	9.5	0.79	8.2	-0.30
PS07	406	122.4	76.4	79	63	-1.47	34.01	10.2	0.84	8.3	-0.51
KD 05	41	126.0	76.8	51	50	-1.78	33.56	12.5	0.51	4.4	-1.40
KD 06	1	125.9	76.7	63	56	-1.36	33.95	12.1	0.83	7.7	-0.40
VB07	1	125.9	76.7	~ 70	60	-1.50	33.97	9.7	0.71	8.2	-0.54
IP07-2	4L_1	125.9	76.7	62	60	-1.56	33.89	13.6	0.80	6.5	-0.63
IP07-2	4L_5	125.9	76.7	62	50	-1.61	33.77	10.8	0.78	7.9	-0.68
IP07-2	4L_9	125.9	76.7	62	40	-1.68	33.59	11.8	0.77	6.6	-0.97
IP07-2	4L_9	125.9	76.7	62	60	-1.54	33.92	8.8	0.82	14.2	-0.63
IP08-2	193M	126.1	76.6	52	40	-1.48	33.13	11.2	0.23		-1.59
VB07	54	130.5	77.2	~ 70	63	-1.53	33.92	10.3	0.74	7.4	-0.64
KD 05	30	144.0	79.0	90	50	-1.44	33.35	10.8	0.92	5.8	-1.17
KD 06	11	144.0	79.0	90	80	-0.91	34.16	8.7	0.74	7.6	-0.39
IP07-2	10	143.0	78.5	68	65	-1.53	33.60	11.8	0.90	8.8	-1.04
IP08-2	201M	143.0	78.0	50	48	-1.57	32.1	16.0	0.04		-2.73

Halocline water modification and along slope advection

D. Bauch et al.

Table 3. Property ranges of water masses in the upper 100 m of the water column at the Laptev Sea continental margin (compare Fig. 6).

	Laptev Sea central shelf bottom waters at 25–50 m	cont. slope at ~ 126° E slope water at 50–80 m	basin at ~ 126° E LHW at 25–50 m	basin ~ 142° E LSHW at 25–50 m
f_{SIM} [%]	~ -10	~ -4 to 0	~ -2 to -5	~ -2 to -7
Si [$\mu\text{mol kg}^{-1}$]	15 to 100	10 to 12	2 to 6	4 to 10
S	31.5 to 32.5	33.1 to 33.9	33.1 to 33.8	31.4 to 33.7
T [°C]	~ -1.6	~ -1.5 to -1.3	~ -1.7	~ -1.7 to -1.5

Title Page

Abstract

Introduction

Conclusions

References

Tables

Figures

◀

▶

◀

▶

Back

Close

Full Screen / Esc

Printer-friendly Version

Interactive Discussion



Halocline water modification and along slope advection

D. Bauch et al.

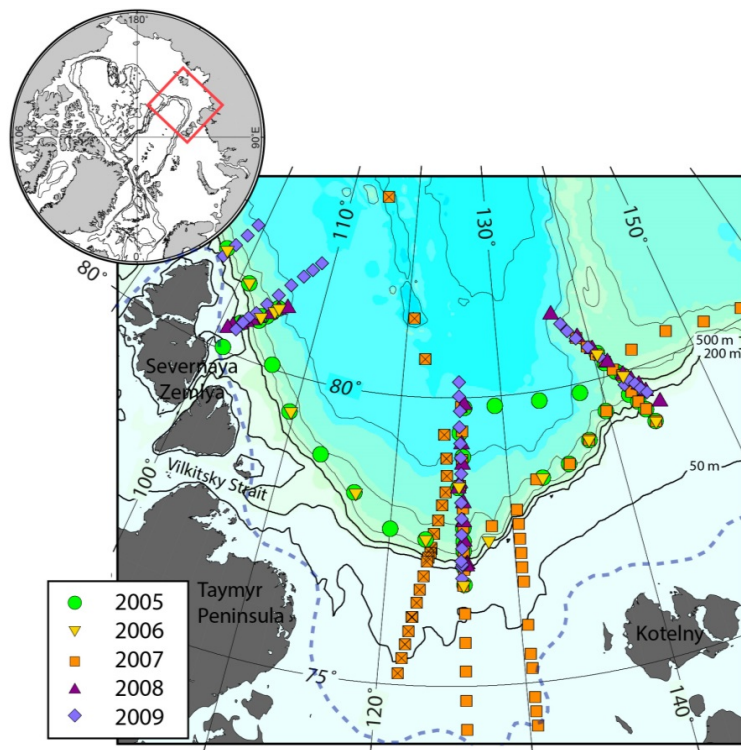


Fig. 1. Geographical distribution of stations near the Laptev Sea continental slope. Shown are all stations from NABOS expeditions taken in summers 2005 to 2009 and during Polarstern expedition PS07 taken in summer 2007 (additionally marked with a cross). Black solid lines show the position of the 500, 200 and 50 m isobaths that indicates the shelf break, and mark the northern borders of the outer and central Laptev Sea shelf, respectively. The stippled line marks the average position of the fast ice edge. Between pack ice and fast ice edge flaw polynyas are formed during winter (e.g., Krumpfen et al. 2013).

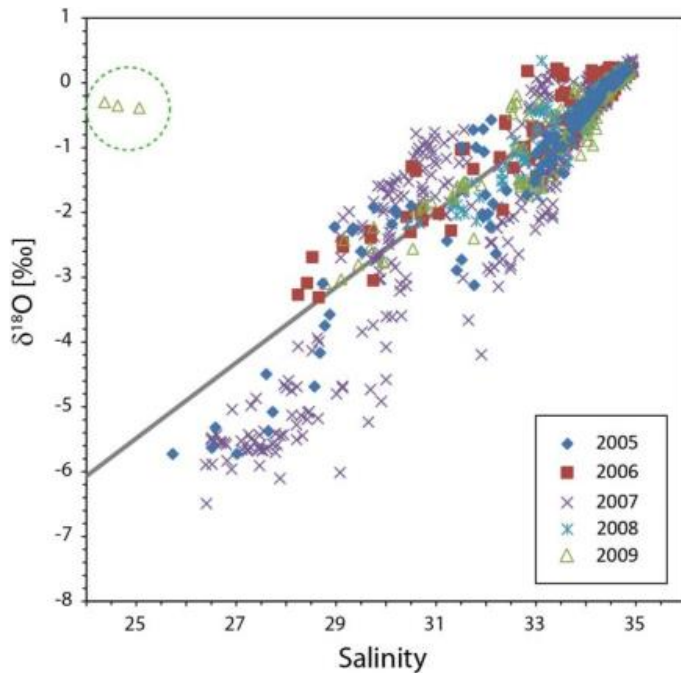


Fig. 2. $\delta^{18}\text{O}$ versus Salinity in the upper 150 m of the water column for data taken during NA-BOS 2005–2009 and PS07 near the Laptev Sea continental slope (Fig. 1). The direct mixing line between Atlantic water and river water endmembers (see Table 1) is shown in gray for reference. The stippled circle highlights anomalous data from the upper 30 m from a station north of Severnaya Zemlya (KD-67-09; 101.8° E, 80.4° N).

Halocline water modification and along slope advection

D. Bauch et al.

Title Page

Abstract Introduction

Conclusions References

Tables Figures

⏪ ⏩

◀ ▶

Back Close

Full Screen / Esc

Printer-friendly Version

Interactive Discussion



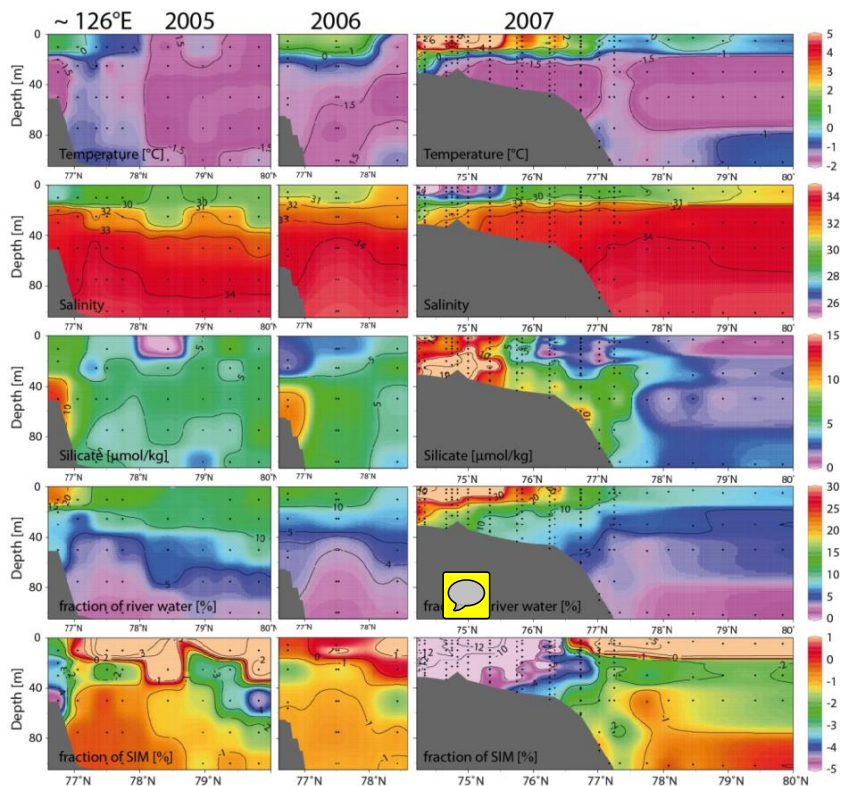


Fig. 3. Oceanographic sections along 126°E taken in summers 2005–2009 based on NABOS 2005–2009, TRANSDRIFT 2007–2009 and PS07 data. Shown are Temperature, salinity, silicate concentration and $\delta^{18}\text{O}/\text{S}$ derived fractions of river water and sea-ice meltwater. Note that negative fractions of sea-ice meltwater represent the amount of freshwater removed as sea-ice and are proportional to the amount of brine added to the water parcel. For further explanation see text.

Halocline water modification and along slope advection

D. Bauch et al.

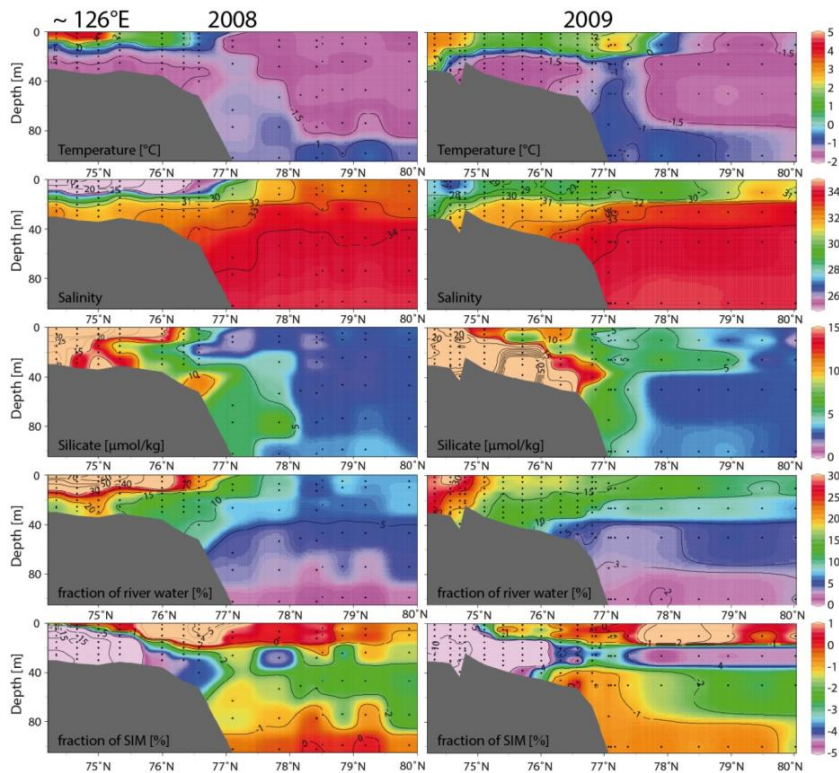


Fig. 3. Continued.

Title Page

Abstract

Introduction

Conclusions

References

Tables

Figures

◀

▶

◀

▶

Back

Close

Full Screen / Esc

Printer-friendly Version

Interactive Discussion

Halocline water modification and along slope advection

D. Bauch et al.

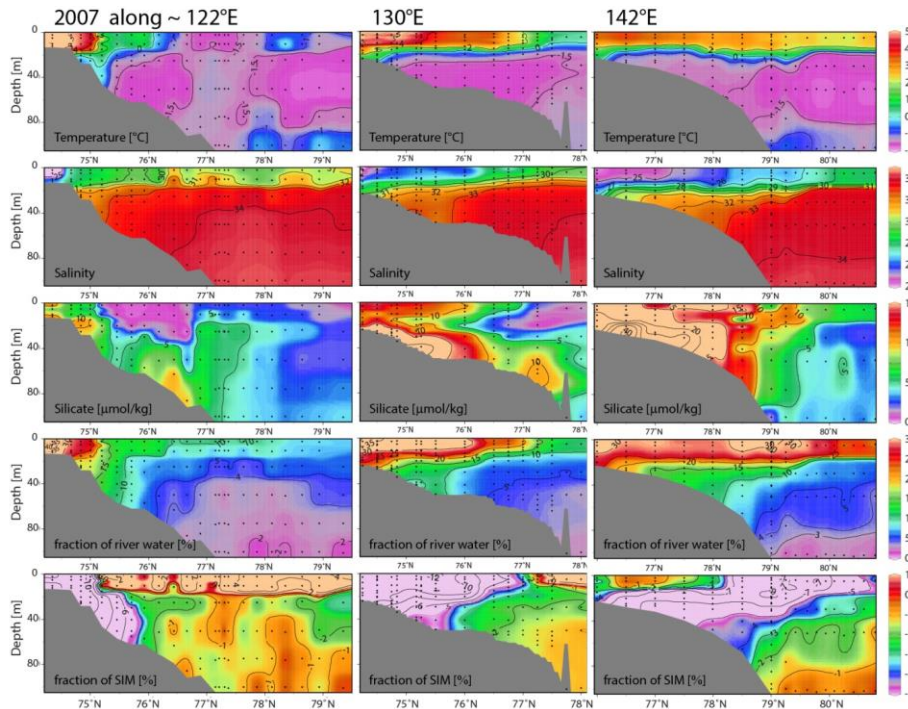


Fig. 4. Oceanographic sections taken in 2007 along $\sim 122^\circ$ E (left), 130° E (middle) and $\sim 142^\circ$ E (right) (note that the section taken at 126° E in 2007 is shown in Fig. 3). Sections are based on IP07, VB07 and PS07 data.

Title Page

Abstract

Introduction

Conclusions

References

Tables

Figures

◀

▶

◀

▶

Back

Close

Full Screen / Esc

Printer-friendly Version

Interactive Discussion

Halocline water modification and along slope advection

D. Bauch et al.

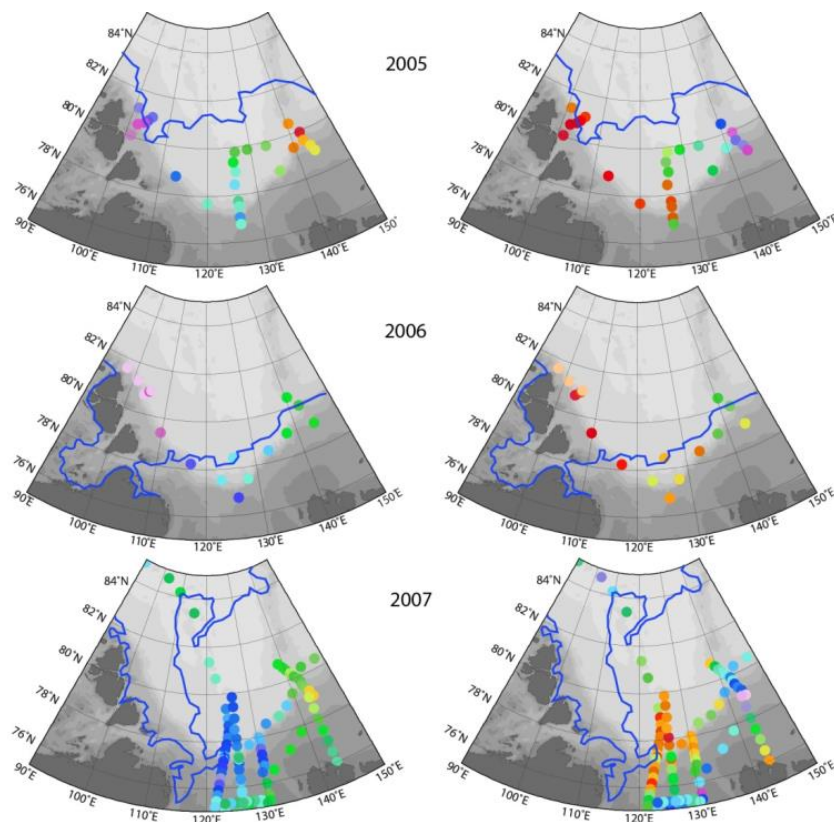


Fig. 5. Integrals of river and sea-ice meltwater fractions over the upper 150 m of the water column. Also shown in blue is the sea-ice edge on 15 September based on daily sea-ice concentration data from Bremen University (Advanced Microwave Scanning Radiometer-EOS (AMSR-E); Spreen et al., 2008).

[Title Page](#)[Abstract](#)[Introduction](#)[Conclusions](#)[References](#)[Tables](#)[Figures](#)[◀](#)[▶](#)[◀](#)[▶](#)[Back](#)[Close](#)[Full Screen / Esc](#)[Printer-friendly Version](#)[Interactive Discussion](#)

Halocline water modification and along slope advection

D. Bauch et al.

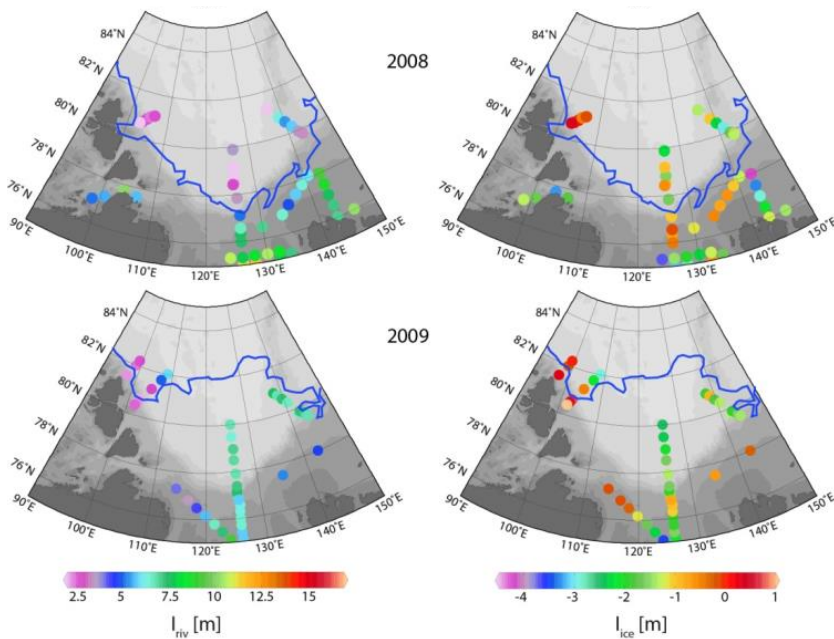


Fig. 5. Continued.

[Title Page](#)[Abstract](#)[Introduction](#)[Conclusions](#)[References](#)[Tables](#)[Figures](#)[◀](#)[▶](#)[◀](#)[▶](#)[Back](#)[Close](#)[Full Screen / Esc](#)[Printer-friendly Version](#)[Interactive Discussion](#)

Halocline water modification and along slope advection

D. Bauch et al.

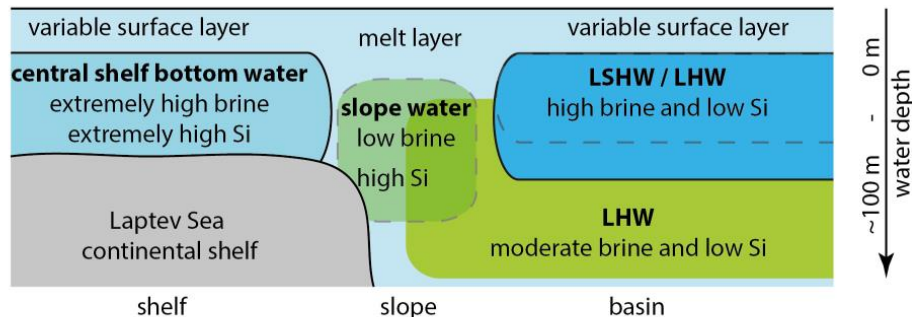


Fig. 6. Sketch of the water mass structure within the halocline on a section across the Laptev Sea continental shelf and slope into the Eurasian Basin. LSHW refers to Low-Salinity Halocline Water with $S < 33$ that is predominantly found east of 130°E . LHW refers to Lower Halocline Water with $S \sim 33\text{--}34.5$ that also contains a brine signal at $S > 33$. For further explanation see text.

Title Page

Abstract

Introduction

Conclusions

References

Tables

Figures

◀

▶

◀

▶

Back

Close

Full Screen / Esc

Printer-friendly Version

Interactive Discussion



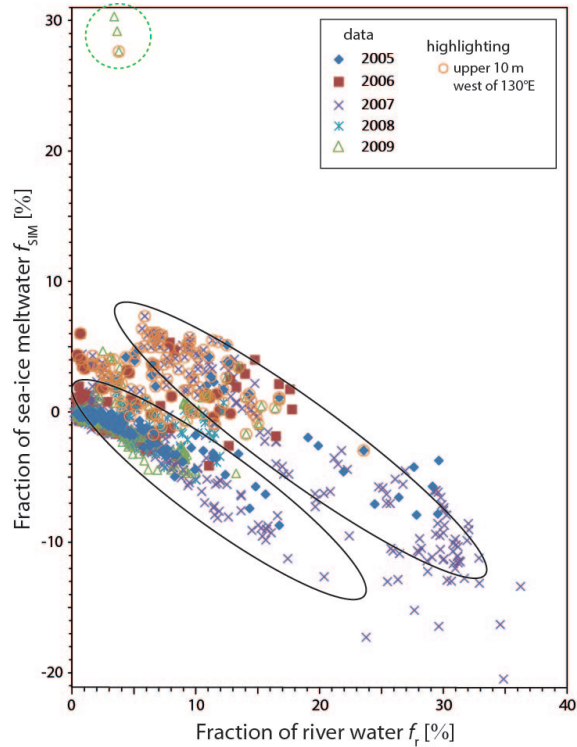


Fig. 7. Fractions of sea-ice meltwater (f_{SIM}) versus fractions of river water (f_r) for the upper 150 m of the water column for NABOS 2005–2009 and PS07 data at the Laptev Sea continental margin (Fig. 1). Clusters within f_{SIM}/f_r correlations are highlighted with ellipses. Orange circles highlight the upper 10 m on the western Laptev Sea slope (west of 130° E and north of 76.5° N). The stippled circle highlights anomalous data from the upper 30 m from a station north of Severnaya Zemlya (KD-67-09; 101.8° E, 80.4° N; samples were taken at 5, 11 and 26 m water depth; CTD data show a sharp increase in salinity, with ~ 25 at 0–34 m to 28 at 35 m, and 34 at 36 m).

Halocline water modification and along slope advection

D. Bauch et al.

Title Page

Abstract Introduction

Conclusions References

Tables Figures

⏪ ⏩

⏴ ⏵

Back Close

Full Screen / Esc

Printer-friendly Version

Interactive Discussion



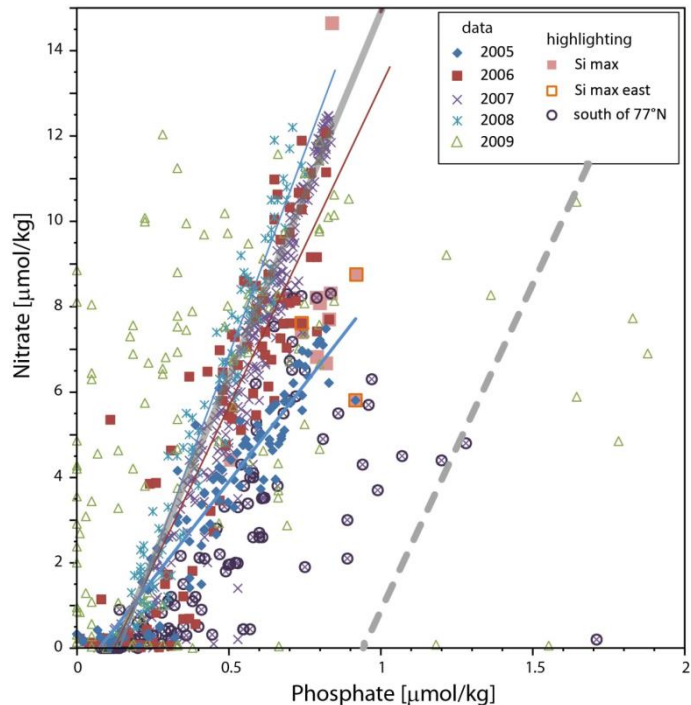


Fig. 8. N/P correlation for the upper 150 m of the water column for NABOS 2005–2009 and PS07 data at the Laptev Sea continental margin (Fig. 1). Indicated are pure Atlantic N/P relation (solid gray line with $N = 16.785 \cdot P - 1.9126$ after Bauch et al., 2011b) and for reference, also the pure Pacific N/P relation is shown (stippled line with $N = 15.314 \cdot [PO_4] - 14.395$ after Jones et al., 2008). Also indicated are linear correlations for datasets taken in 2005, 2006 and 2008 in corresponding colours. Linear correlation for 2007 shelf break data is identical to the Atlantic N/P relation. Note that data from 2005 show a systematic deviation from the Atlantic Water N/P correlation, that we believe to be a systematic error in N measurements. N/P values from 2009 data show unsystematic scatter and are disregarded.

Halocline water modification and along slope advection

D. Bauch et al.

Title Page

Abstract Introduction

Conclusions References

Tables Figures

⏪ ⏩

⏴ ⏵

Back Close

Full Screen / Esc

Printer-friendly Version

Interactive Discussion



Halocline water modification and along slope advection

D. Bauch et al.

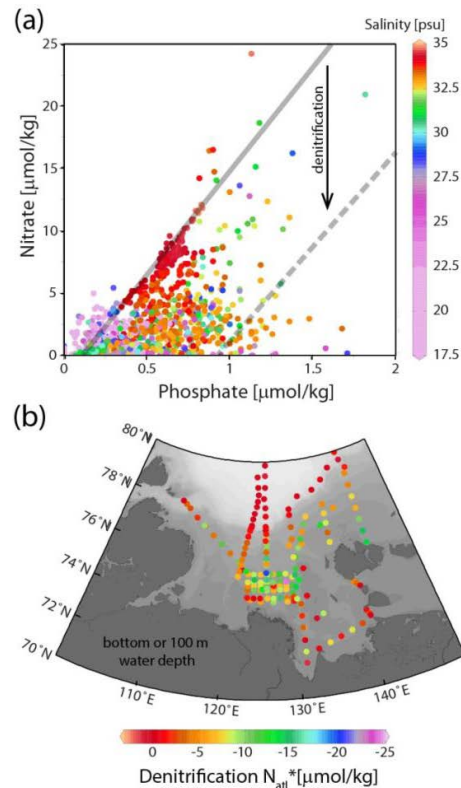


Fig. 9. (a) Nitrate versus phosphate for shelf waters and upper 100 m for stations taken during PS07 and VB07 in summer 2007 (upper panel). The salinity of each sample is indicated by colouring. The grey line shows the Atlantic N/P relation. **(b)** Denitrification signal N_{Atl}^* calculated as deviation relative to the Atlantic N/P relation ($N_{\text{Atl}}^* = N - 16.835 \cdot P + 1.918$) for bottom waters or 100 m water depth. Note that N_{Atl}^* is similar to N^* calculated after Gruber and Sarmiento (1997) relative to global N/P values. For further explanation see text.